

## 전해 석출 기술의 최근 개발 동향

김선규, R.G. Reddy\*

울산대학교 첨단소재공학부 \* 알라바마대학교 금속및재료공학과

## Recent Advances in Electrodeposition Technology

S. K. Kim and R. G. Reddy\*

School of Materials Science and Engineering, University of Ulsan, Ulsan, Korea 680-749

\* Department of Metallurgical and Materials Engineering  
 The University of Alabama, Tuscaloosa, AL 35487-0202, U.S.A.

### Abstract

Electrodeposition technology is widely used in industry for various kinds of coatings. Modifications in this technology led to several processes to meet various requirements. Electrolysis in ionic liquids has many advantages such as low energy consumption of energy, low pollutant emission and low operating costs. Although ionic liquids have already been used in liquid/liquid extraction processes, only recently their use in electrodeposition was exploited. Electrochemical deposition of composites is an expanding area. Coupled with the progress in the synthesis of nanometric powder, this research will open a large number of innovative materials. Pulse current plating is another electrodeposition technique which yields improved coatings. Although electrodeposition is now regarded as an environmental non-friendly process, it is economically viable and has many inherent advantages. For certain applications, alternatives to electrodeposition have not yet been fully implemented. Hence, continued research in this technology is warranted. This article reviews some recent advances in electrodeposition technology. Aspects of electrodeposition such as electrolysis in ionic liquids, electrodeposition of composites, pulse current plating techniques, metal and alloy deposition, compound deposition and effects of additives are discussed in this review.

### INTRODUCTION

Electrodeposition is being used traditionally for decorative, corrosion and wear resistant coatings as well as in electronic industries. This process is now regarded as pollutant generator. Recently,

alternate processes which are environmentally friendly, such as ion plating and sputtering are being sought. However, electrodeposition technology has many inherent advantages such as fast deposition, mass production and cost effectiveness. Electrodeposition of sheets for automotive

application and printed circuit boards in electronic industries are good examples where electrodeposition technology has not been replaced. Therefore, continued efforts should be directed toward this important technology. In this paper, some recent advances in electrodeposition are reviewed.

### ELECTROLYSIS IN IONIC LIQUIDS

In this section, novel application of ionic liquids in the electrodeposition and refining technologies is discussed

Ionic liquids are mixture of inorganic and organic salts which are liquid at room temperature and have wide temperature range. Ionic liquids are suitable electrolytes for electrodeposition owing to the properties such as wide electrochemical windows, stable chemical properties, extreme low volatility, and nonflammability. The application of ionic liquids in aluminum reduction and refining were reported. The results indicated several advantages such as low consumption of energy and electrode materials, low pollutant emission, and low operating costs over conventional processes for aluminum reduction and refining. Wu et al.<sup>1)</sup> studied the use of ionic liquids in the reduction of aluminum via electrolysis at ambient temperatures. Anhydrous aluminum chloride was used as raw material. The electrolyte was made from  $\text{AlCl}_3$  and 1-*n*-butyl-3-methylimidazolium chloride. Aluminum was deposited at the copper cathode and chlorine gas was evolved at the graphite anode. Experimental temperatures were in the range of 100~140°C. Cathode current density was 200~700  $\text{A}/\text{m}^2$ . Dense aluminum deposition of 0.1~0.2 mm thick was obtained.

Wu et al.<sup>2)</sup> also carried out experiments on aluminum refining via electrolysis using ionic liquids at 105 °C. mpure aluminum was dissolved at the anode and pure aluminum (>99.9%) was deposited at the copper cathode. SEM micrograph of dense aluminum deposit on copper cathode is shown in Fig. 1. Current density of 310 ~ 730  $\text{A}/\text{m}^2$  and current efficiency of about 99% were obtained. Impurities such as Si, Cu, Zn, Fe, Mg, Cr, Ni, Mn and Pb were removed as anode residue. The energy consumption of about 3kWh/kg-Al was obtained at a cell voltage of about 1 V. In comparison with the conventional industrial refining process, electrorefining using ionic liquids has advantages of low energy consumption and low pollutant emission.

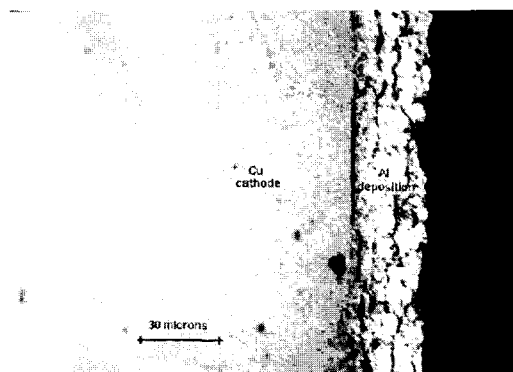


Fig. 1. SEM micrograph of aluminum deposit on copper cathode.

Liao et al.<sup>3)</sup> investigated the constant current electrodeposition of bulk aluminum on copper substrate in the Lewis acid, 50 mol.% aluminum chloride-1-methyl-3-ethylimidazolium chloride room temperature molten salt. The quality of the electrodeposit was greatly enhanced by the addition of benzene as a 'cosolvent.' Electrodeposits produced in such melts exhibited a grain size on the order of 5 to 15  $\mu\text{m}$ . Chen et al.<sup>4)</sup> investigated

the electrodeposition of copper and copper-zinc alloys on tungsten and nickel electrodes in a Lewis acid, 50 mol.% zinc chloride - 1-ethyl-3-methyl/imidazolium chloride molten salt containing copper(I). The composition of electrodeposited Cu-Zn alloys was varied by varying deposition potential, temperature, and Cu(I) concentration of the plating bath.

### ELECTRODEPOSITION OF COMPOSITES

In this section, electrodeposition of multilayered composites is discussed. Typically, a composite layer comprises of metal matrix such as nickel and dispersion of ceramic particles such as SiC or polymer particles such as Teflon. Electrochemical deposition of composites is an expanding subject in electrochemical materials science. In order to better cope with the requirements of new application fields, new dispersion materials like polymers, oxides and electrochromic salts have been tested

Kim and Yoo<sup>5)</sup> reported the formation of bilayer Ni-SiC composite coatings by electrodeposition. By manipulating the current density and the plating time properly, they were able to produce gradient Ni-SiC composite layers. Fig. 2 shows SEM micrograph of the bilayer Ni-SiC composite coating. The inner layer consists of sparsely distributed SiC particles in nickel matrix whereas outerlayer was more dense in SiC. Formation of gradient composite layers on tool steel enables smooth transition of composite microstructure which yields better mechanical properties when compared to a single dense Ni-SiC layer. Although this work reports results on bilayer composite coating, this technology could be extended to form multilayers to further improve the properties

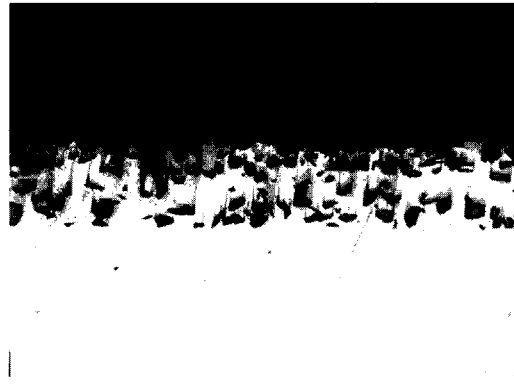


Fig. 2. SEM micrograph of the bilayer Ni-SiC composite Coating

of coatings. Guo and Zhu<sup>6)</sup> reported the electrodeposition of Ni-W-SiC composite deposits. Results showed that the alloys containing more than 44 wt.% W content and the composite deposits containing 7.8 wt.% SiC can be obtained. Alloys and their composite deposits with over 44 wt.% W content show amorphous structure. The hardness of amorphous Ni-W alloys and their composite deposits increase when they are heated and can reach 1350 HV and 1520 HV respectively for 46 wt.% W content. The adhesion on copper, carbon steel and stainless steel were all very good.

The use of electrochemical impedance spectroscopy (EIS) for the in situ control of the electrolytic codeposition of Ni-SiO<sub>2</sub> and Ni-SiC was investigated by Nowak et al.<sup>7)</sup> SiC particles that are being embedded in the growing metal layer cause an apparent decrease in the electrode surface area. In the case of SiO<sub>2</sub> particles, which were embedded in the metal matrix to a very limited extent, caused an apparent increase in the electrode surface area. Relationship of the electroplating on the composition, structure, surface appearance of the Ni-W-ZrO<sub>2</sub> amorphous composite films with ZrO<sub>2</sub> particles were studied by Zhu

and Li.<sup>8)</sup> The results show that the Ni-W-ZrO<sub>2</sub> amorphous composite films show a good oxidation resistance during the heat treatment at 500°C for 50 h. Moeller and Hahn<sup>9)</sup> synthesized and characterized nanocrystalline Ni-ZrO<sub>2</sub> composite coatings. Nanocrystalline ceramic powders with grain size below 10 nm were suspended in the plating solution and the ceramic particles codeposit with the metal to produce nanocrystalline metal matrix composite coatings. The influence of the plating parameters on the content and dispersion of the codeposited ceramic particles was investigated. The experimental results were correlated to the mechanical properties of the coatings. Nanocrystalline Ni- composite films were formed by codeposition of Ni and  $\gamma$ -Al<sub>2</sub>O<sub>3</sub> nanoparticles in electrolytic plating baths by Mueller and Ferkel.<sup>10)</sup> Nanoscaled ceramic particles produced via laser ablation technique with a median particle diameter of 14 nm or commercial available particles produced via physical vapor synthesis process with a median particle diameter of 25nm were dispersed in a sulfamate bath followed by D. C. electroplating.

Barmak et al.<sup>11)</sup> produced multilayered coatings of single and dual particle metal matrix composites, with or without ceramic overlayers by a novel combination of electrochemical deposition (electroplating and electrophoretic deposition) and reaction bonding. The coatings contained the following layers in a variety of combinations deposited on Ni substrates: (i) electrodeposited composites of Ni with Al and/or alumina particles, (ii) Al+Al<sub>2</sub>O<sub>3</sub>+yttria stabilized ZrO<sub>2</sub> transformed into Al<sub>2</sub>O<sub>3</sub>+yttria stabilized ZrO<sub>2</sub> by reaction bonding method, and (iii) yttria stabilized ZrO<sub>2</sub>. In order to determine the appropriate processing

parameters for the multilayered coatings, uniform single layer coatings were deposited and characterized. They found that in the dual particle Ni-Al-Al<sub>2</sub>O<sub>3</sub> coatings the volume percent of the particle did not show a dependence on deposition current density. However, volume percent of alumina in these coatings had a strong dependence on the alumina content of the plating bath, while the volume percent of Al showed only a weak dependence on its content of the bath. Comparison of the deposition behavior of these dual particles with that of single particle coatings containing Al or alumina revealed that the presence of Al in the bath interferes with the codeposition of alumina. When coatings containing Al were annealed, Ni and Al reacted to form a solid solution of Al in Ni ( $\gamma$ ) or a two phase mixture of this solid solution and the intermetallic, Ni<sub>3</sub>Al, ( $\gamma$ - $\gamma'$ ) depending on the annealing temperature. Also, they found that the formation of the reaction bonded alumina and yttria stabilized zirconia layer requires the oxidation resistance afforded by aluminum in the underlying electroplated layer.

Switzer et al.<sup>12)</sup> investigated electrodeposition of nanocomposite films of copper metal and cuprous oxide at room temperature from an alkaline copper (II) lactate solution. The electrode potential oscillated spontaneously during constant-current deposition of the composites. The oscillations were periodic in a stirred solution, but became chaotic in unstirred solution. For a given current density, the phase composition was a strong function of solution pH. As the pH increased, the cuprous oxide content increased. At pH 12, no oscillations were observed, and pure cuprous oxide was deposited

Onoda et al.<sup>13)</sup> electrodeposited Ni-B alloy films

using a rotary electrode under various plating conditions and investigated the mechanism of the codeposition of B into the deposits. Use of a rotary electrode expands the useful current density regions compared to a static bath. The deposition rate of B was related to the thickness of the diffusion layer at the cathode surface. The electrodeposition of AuCu-B<sub>4</sub>C composite from alkaline bath containing free cyanide was studied by Bozzini et al.<sup>14)</sup>. The electrochemical behavior of the bath and the metallographic and crystalline structures of the electrodeposited alloys were studied with and without addition of B<sub>4</sub>C particles. Electrochemical instabilities were observed and their influence on the structure of both pure matrix and composite electrodeposits was investigated.

Taterina and Khaldeev<sup>15)</sup> proposed acetate electrolytes for the production of corrosion and abrasion resistant nickel-Teflon composites. The electrolytic parameters are optimized for the production of high quality composites. A parallel plate flow cell was designed for the study of polymer particle codeposition in metal electrodeposition by Filiatre and Towarnicki<sup>16)</sup>. The effects of two surfactants (anionic sodium dodecyl sulphate and cationic cetyl trimethyl ammonium bromide) on the adhesion of anionic polystyrene particles to a nickel substrate were examined. The deposition rate in laminar flow was measured. The adsorption of sodium dodecyl sulphate and cationic cetyl trimethyl ammonium bromide on both electrode and the particles and its effect on changes of the interaction potential at a short distance was discussed.

## PULSE CURRENT PLATING

In this section, the use of pulse current electrodeposition is discussed. Electrodeposition by pulsed current is a subject of continued interest. Varadarajan et al.<sup>17)</sup> investigated electrodeposition of copper into about 0.25  $\mu\text{m}$  trenches by pulse plating. Deposit evolution inside trenches was studied. Copper deposits with good morphology and resistivity were obtained using the alkaline bath. They also developed a two-dimensional pseudo-steady state and a one-dimensional unsteady-state mass-transfer models to study the effect of important parameters on the step coverage, evolution of copper deposits and the deposition rate. Model predictions were in good agreement with the experimental results. Periodic pulse reverse (PPR) plating was introduced as an improved processing technique for acid-copper plating. This technology can provide uniform plating at relatively high current densities. Blake et al.<sup>18)</sup> reported optimization of microvia plating based on the method of plating, direct current vs. PPR, and the positioning of the fluid delivery system.

Ghosh et al.<sup>19)</sup> studied the effect of pulse parameters on the composition of Ni-Cu alloys deposited from a citrate bath. Coherent, smooth and bright coating was obtained by precise control of the pulse time, relaxation time and peak current density. Stirring, high pH and high temperature was shown to increase the copper content of the deposit. The deposited Ni-Cu alloy was nanocrystalline (crystallite size approximately 2.5~28.5 nm) and it existed in a single FCC-phase. The corrosion resistance of the pulse-plated Ni-35.8 wt.% Cu alloy, as evaluated by potentiodynamic

method, was better than that of the D. C.-plated alloy and the commercial Monel-400.

Panagopoulos et al.<sup>20)</sup> investigated the possibility of producing multilayered alloy coatings consisting of alternate amorphous layers, by the electrodeposition using pulsed current. The alternate metallic amorphous layers were selected to consist of Ni-P-W ternary alloys, in order to study the effect of the incorporation of a third element in the structure of an electrodeposited Ni-P multilayered alloy coating. The well-defined layered structure found in the Ni-P-W multilayered alloy coating, consisting of X-ray amorphous layers, show that production of a ternary Ni-P-W multilayered alloy coating with the selected method was feasible and this might expand the potential applications of a Ni-P based multilayered alloy coating.

The morphology of Zn-Co electrodeposits obtained by pulsed current plating was studied by Tomachuck et al.<sup>21)</sup> The plating bath was an acid bath containing chloride ions. The results showed that pulsed current deposition favors the production of deposits with better adhesion, homogeneity and having a lower porosity than those obtained with direct current. The morphology of the deposits depended on deposition parameters but not on cobalt content of the deposit.

Robin and Ribeiro<sup>22)</sup> carried out electrodeposition of titanium in the  $K_2TiF_6$ -LiF-KF melt using both direct and unipolar pulse current techniques. Dense and smooth titanium coatings were obtained by pulse current plating at 750°C. The cathodic current efficiency was in the range of 60~65%. Ett and Pessine<sup>123)</sup> obtained uniform and very low porous  $TiB_2$  coating deposition using continuous current plating and pulse current plating,

electrochemical techniques. The solvent used is a fluoride mixture (LiF-NaF-KF) with solutes  $K_2TiF_6$  and  $KBF_4$  in a mass relation of one to four after treatment to remove moisture. The temperature was 600°C and graphite electrodes were used as substrates.

## METAL AND ALLOY DEPOSITION

Portela et al.<sup>24)</sup> Studied copper electrodeposition on platinum electrodes from slightly acidic solutions of copper sulfate containing nicotinic acid (NA). NA produced an inhibition of the copper deposition. Complex species formation between NA and cuprous ions occur at the interface. NA acid acts as a very effective brighter producing highly uniform and smooth surfaces of copper deposits. Moffat et al.<sup>25)</sup> demonstrated superconformal electrodeposition of copper in 500 nm deep trenches ranging from 500 to 90 nm width using an acid cupric sulfate electrolyte containing chloride, polyethylene glycol and 3-mercapto-1-propanesulfonate.

Georgiadou et al.<sup>26)</sup> studied shape evolution during electrodeposition of copper in microtrenches numerically by a model which incorporates adoptive meshing capabilities. Filling trenches with copper without creating void was related to plating additives in solution. The shape-change behavior of this system resulting from variation of the feature's aspect ratio, bulk composition, and level of additive components were investigated. The operating window of bath compositions for void-free electrodeposition was studied in the range of  $0.25 \times 10^{-4}$  to  $10^{-4}$  M bulk concentration of additive in a 0.25 M  $CuSO_4$  + 0.2 M  $H_2SO_4$  plating solution and for aspect ratios from 0.5 to 4.

Arai et al.<sup>27)</sup> investigated electrodeposition of Sn-Cu alloy for use as Pb-free soldering. Pyrophosphate bath containing potassium iodide was used as a basic Sn-Cu alloy electroplating bath. Polyethylene glycol (mean molecular weight = 600 : PEG600) and formaldehyde were used as additives. Electrochemical behavior, composition of electrodeposits, surface morphology and phase structure were studied. Copper content in deposits decreased with increasing current density and Sn-Cu alloys with the composition near the eutectic composition (Sn-1.3 at.% Cu) were obtained in the range of current densities from 1 to 2 A dm<sup>-2</sup>. Dull Sn-Cu alloy was electrodeposited from the basic bath and the bright Sn-Cu alloy was obtained from the bath modified by adding both formaldehyde and PEG600 to the basic bath. It is suggested that the process of the reductive decomposition of formaldehyde on the alloy electrodeposit related to the smoothing of Sn-Cu alloy films.  $\beta$ -Sn phase only or two phases of  $\beta$ -Sn phase and n phase (Cu<sub>6</sub>Sn<sub>5</sub> phase) were observed with the electrodeposited Sn-Cu alloys.

Ebrahimi and Liscano<sup>28)</sup> made laminated Ni/Cu structures by electrodeposition using a single bath sulfamate solution. The texture of deposits was found to depend on their thickness, purity of the electrolyte and its copper content, deposition temperature and the bi-layer thickness. The deformation and fracture of these structures were characterized by testing free-standing tensile specimens. The fracture behavior varied drastically among the specimens from so-called knife-edge behavior to complete cleavage-like fracture. The purity of the solution and nodule formation was found to be the most important factors that affected the ductility of the deposits. The obser-

vations made in this study suggest that co-deposition of hydrogen is responsible for the embrittlement of specimens produced from impure electrolytes.

Shawki and Mikhail<sup>29)</sup> produced black nickel alloy coatings suitable for solar collectors by electrodeposition from baths containing Ni and Zn sulfates and thiocyanate. Variables having the greatest influence on optical properties of the black deposits were : pH-value, temperature, zinc and thiocyanate concentration. Of particular importance was the plating current which was related to the cathode potential that controlled the composition, and alternatively, the optical properties of the deposited coatings. The mechanism of blackening of the Ni coatings was attributed to the deposition of sulfide particles with Ni-Zn alloy. It was shown that, in absence of thiocyanate co-deposited Zn caused a degree of blackening to Ni coatings due to the deposition of Ni<sub>2</sub>Zn<sub>22</sub> as identified by x-ray phase analysis. Considerable blackening could be achieved by sulfur, which was deposited as Ni<sub>3</sub>S<sub>2</sub>. In a modified composition it was possible to replace sulfur by phosphorous supplied to the coating by the addition of sodium hypophosphite to the plating solution. The coatings were of optimum optical properties as far as maximum absorptance and minimum emittance. Absorptance values as high as 0.93 could be obtained for selective coatings (2-3 microns thick) deposited under optimized conditions. Performance tests for coated solar water heater panels showed that the coatings are well qualified. The endurance of the coatings was evaluated in actual service conditions with regard to thermal degradation and corrosion resistance.

Yamasaki<sup>30)</sup> showed that nanocrystalline Ni-W

alloy with high tensile strength of about 2300 MPa with good ductility could be produced by electro-deposition. The embrittlement behaviors of the Ni-W electrodeposits during annealing were studied. A mechanism for embrittlement during grain growth in nanocrystalline materials was discussed.

Goldbach et al.<sup>31)</sup> investigated Ni-Co deposition from a sulfamate bath in the presence of boric acid and two additives. The individual deposition of nickel was shown to be partly inhibited by the adsorption of sulfamate ions at low polarization; such inhibition was not observed for cobalt. The introduction of saccharin at 100 ppm, with a wetting agent seemed to hinder sulfamate adsorption and Ni deposition departed at less cathodic potentials. The presence of cobalt had no effect on nickel deposition, whereas cobalt deposition was hindered by the presence of nickel in the bath. Galvanostatic deposition was carried out at the surface of a rotating disc electrode and with a rotating cylinder Hull cell. At low current densities deposits with a Co content of approx. 40% were produced, but this content was shown to decrease with the applied current density. Examination of experimental data showed that cobalt deposition was diffusion-controlled and that Co content decreased with the applied current density relative to the limiting current density.

Donten et al.<sup>32)</sup> studied electrodeposition of thin layers of a new amorphous alloy, Fe-Ni-W. The iron mole fraction,  $[Fe]/([Fe] + [Ni])$ , was changed from 0 to 1. However, the best properties under constant current deposition were obtained for the mole fraction near 0.5. The key, needed properties of the Fe-W and Ni-W alloys were transferred to the Fe-Ni-W alloy, while the

unwanted properties of the two-component alloys were eliminated. The new alloy was hard (1040 HV, for equal percentage of Fe and Ni), smooth, of nice appearance, and of good adherence to both steel and copper. Pulse electroplating further improved the smoothness and uniformity of the electrodeposited layers and allowed one to obtain higher tungsten content of up to 35 at. %.

Giz et al.<sup>33)</sup> reported electrodeposition of NiFe-Zn alloys NiFeZn alloys followed by chemical leaching in KOH solution. A sulphate bath was used to electrodeposit the NiFeZn alloys on a mild steel substrate. The evaluation of this material as electrocatalyst for the hydrogen evolution reaction was carried out in alkaline solutions through steady-state polarization curves. The long term operation at  $135 \text{ mA cm}^{-2}$  showed good stability for up to 200 h. A positive aspect of this cathode is that the polarization behavior of the material shows one Tafel slope over the temperature range 25-80 °C. The operational potential of the material in 28% KOH at 80 °C is about 100 mV which is significantly lower than that of mild steel (400 mV).

Zhuang and Podlaha<sup>34)</sup> examined the anomalous electrodeposition of NiCoFe ternary alloys. Ni deposition in the ternary system appeared inhibited compared with its single-metal deposition, which characterized typical anomalous behavior. Fe deposition was enhanced, similar to recent findings in codeposited binary alloys. Both catalytic and inhibiting effects were observed for Co deposition. The inverse Tafel slopes for both the metal reduction reactions and the side reactions were determined and compared with the values obtained during the single-metal reductions. A common change in the inverse Tafel slopes sug-



gested a dependent kinetic relationship between the metal and side reaction rate during NiCoFe alloy deposition.

Barrera et al.<sup>35)</sup> evaluated cobalt electrodeposition on a stainless steel from 1.17 M Co(II) aqueous solution containing 0.98 M H<sub>2</sub>SO<sub>4</sub>, 0.56 M KCl, and H<sub>3</sub>BO<sub>3</sub> in the absence (i) and presence (ii) of 0.1 M KNO<sub>3</sub>. Cobalt electrodeposited from the electrolytic bath (i) was white-gray colored, whereas deposition from bath (ii) formed a black-colored surface. SEM-WDX, AFM, and XRD analysis of the steel surfaces covered with these two deposits revealed distinct characteristics for black and white cobalt films. Although both deposits were composed of metallic cobalt, the white cobalt deposit was a smooth film while the black deposit consisted of many dispersed, nano-sized clusters of 150 to 250 nm in diameter. Analysis of 3D nucleation limited by lattice incorporation of cobalt adatoms to the growth centers. Formation of black cobalt was shown to involve the simultaneous processes of nucleus formation and growth, limited by mass transfer, and the reduction of nitrates in the medium onto the surfaces of these nuclei. It was shown that, beside this cobalt-nitrate interaction, NO<sub>3</sub><sup>-</sup> ions in solution can block active sites for cobalt reduction and the effect of this phenomenon strongly depends on the nitrate concentration. These facts could explain the observed dispersion of the black cobalt coating.

Nikolova<sup>36)</sup> studied the effect of pH and of the time of electrodeposition on the composition and morphology of CoMn layers, obtained at highly negative potentials in the presence of boric acid. Electrodeposition of CoMn at higher pH facilitates in corporation of O and Mn. The coatings underwent substantial changes in composition and mor-

phology in the course of their growth. Gomez<sup>37)</sup> studied the electrodeposition of CoCu alloy on vitreous carbon, copper and nickel electrode in a citrate bath.

Tourillon<sup>38)</sup> reported synthesis of Co and Fe nanowires and nanotubes electrochemically deposited through nonporous membranes. Depending upon the pulse electrodeposition parameters, the structure of Co nanowires is either a pure hexagonal phase or a poly-type structure related to the stacking of hexagonal and face-centered cubic forms. Similarly, iron nanowires can be prepared with single or multocrystallographic phases. Nanotubes whose formation could result from a complexation between metal ion and the polymeric membrane, were also directly synthesized.

Masuda et al.<sup>39)</sup> performed electrodeposition of tungsten and voltammetric experiments in basic ZnCl<sub>2</sub>-NaCl (40-60 mol %) melts containing various tungsten compounds at 450 °C. Gong and Podlaha<sup>40)</sup> studied DC electrodeposition of iron-rich terbium alloys on copper electrodes using aqueous citrate solutions. Bright, gray, thin Fe-Tb alloy films were obtained with low current efficiencies. The result indicated that iron promoted terbium electrodeposition. Lepillar et al.<sup>41)</sup> explored the possibility to increase markedly the electrodeposition rate of cadmium telluride. Results on cell formation with CdS showed that junction formation occurred even for high deposition rates. Efficiencies around 6% (700 mV, 18.1 mA cm<sup>-2</sup>) have been obtained for films grown at 2.7 μm/h.

Thompson et al.<sup>42)</sup> designed a novel platinum electrodeposition technique for preparing catalyst layer in polymer electrolyte membrane fuel cells, which might enable an increase in the level of platinum utilization currently achieved in these

systems. This method consisted of a two-step procedure involving the impregnation of platinum ions into a preformed catalyst layer, followed by a potentiostatic reduction.

Baumgaertner and Gabe<sup>43)</sup> described the development of solutions for palladium alloy electrodeposition outlining the problems of solution chemistry involved. The discussion was focused on the solution formulation for Pd-Fe alloy, as an alternative to Pd-Ni, and the option of considering Co and Ag as further alternatives to Ni. Problems usually encountered in palladium electrodeposition are: hydrogen embrittlement, limited deposition rates, unstable chemical systems, unstable buffer (pH) systems, chemical attack of non-noble metal substrates and high cost of chemistries. To develop viable new palladium or palladium alloy electrolytes, these problems should be considered and solved or their effects must be minimized at least.

Durairajan et al.<sup>44)</sup> showed that an electrodeposited Zn-Ni-Cd alloy coating produced from sulfate electrolyte inhibited the discharge of hydrogen on carbon steel. This ternary alloys had approximately ten times higher corrosion resistance when compared to a Zn-Ni alloy. Hydrogen permeation characteristics of Zn-Ni-Cd alloy coatings were studied and compared with those of a bare and a Zn-Ni alloy coated steel. Various electrochemical properties were obtained by applying a mathematical model to experimental results.

## COMPOUND DEPOSITION

Cao et al.<sup>45)</sup> applied an electrodeposition process to synthesize and deposit  $CN_x$  thin films from

organic solution. The depositions from acetonitrile ( $CH_3CN$ ) and dicyandiamide-acetone ( $C_2H_4N_4 \cdot C_3H_6O$ ) solution were reported. The processes were performed near to room temperature. The films deposited from acetonitrile liquid contained 25% nitrogen, the nitrogen content in the films obtained from dicyandiamide solution reached to 48%. X-ray photoelectron spectrometry (XPS) and Fourier transform infrared (FTIR) were used to characterize the structure of the films.

Albu-Yaron et al.<sup>46)</sup> prepared thin films molybdenum dichalcogenide,  $MoS_2$  by cathodic electrochemical deposition from aqueous and non-aqueous solutions of tetrathiomolybdate ions, at different temperatures. The films were X-ray amorphous as deposited. They were consisted of an amorphous matrix in which quantum sized nanocrystallites or clusters were embedded. Upon annealing at high temperatures, the films obtained from aqueous solutions become crystalline and highly texturized having their van der Waals planes oriented parallel to the substrate, whereas, those obtained from ethylene glycol solutions kept on the amorphous matrix, with slightly larger sizes  $MoS_2$  nanoparticles embedded, than before annealing. Difference in the mechanism of the electrodeposition in aqueous and ethylene glycol solutions was discussed.

Nakamura and Yamamoto<sup>47)</sup> studied electrodeposition of iron and sulfur from an aqueous solution as a method for pyrite ( $FeS_2$ ) thin-film preparation. By using  $FeSO_4$  and  $Na_2S_2O_3$  as source materials, co-deposition of iron and sulfur was attained. Although the S/Fe ratio in deposited films were approximately 1, stoichiometric pyrite thin films were successfully formed by the post annealing at around 500 °C in a sulfur atmosphere.

## EFFECTS OF ADDITIVES

Jung and Lin<sup>48)</sup> studied the rates of Cu deposition from aqueous solutions containing chelating agents, such as citric acid, nitrilotriacetic acid (NTA), and ethylene-diamine-tetraacetic acid (EDTA), in an electrochemical membrane cell. It was shown that the initial rates of Cu deposition decreased in the order citrate > NTA > EDTA, which was not wholly related to the complexing ability of metals and the chelating agents.

Muresan et al.<sup>49)</sup> investigated the effects of some new organic additives, such as horse-chestnut extract (HCE) and a mixture of ethoxyacetic alcohol and triethyl-benzyl-ammonium chloride (IT-85) upon the morphology and structure of copper deposits, as well as upon the cathodic polarization, and compared to those exerted by thiourea and animal glue, in the case of pure, synthetic sulphate solutions. The additive IT-85 was found to be an efficient inhibitor of the copper electro-crystallization process, leading to levelled, fine grained cathodic deposits with a strong [110] texture. The effects of HCE were similar to those exerted by animal glue, leading to deposits consisting of rounded nodules, without a clear texture, reflecting a smaller levelling effect.

Scendo and Malyszko<sup>50)</sup> studied the influence of benzotriazole (BTAH) and tolyltriazole (TTAH) on the cathodic reduction of copper (II) at poly-oriented platinum from acidic chloride solutions by rotating disk voltammetry and cyclic voltammetry combined with electrochemical quartz crystal microbalance (EQCM). The overall electrode process involves two one-electron reactions: Cu(II)/Cu(I) and Cu(I)/Cu, which were characterized by a very large potential separation.

In the additive-free solutions, the first electrode reaction is slightly inhibited by underpotential deposited Cu. On the basis of EQCM results, it was proved that the interaction of BTAH and TTAH with the electrode surface was potential dependent. The adlayers of the inhibitors were removed in the potential range below -0.25 V vs. SCE, in which the adsorption of hydrogen occurred. Consequently, the Cu(II)/Cu(I) electrode reaction was strongly inhibited by BTAH and TTAH while the Cu(I)/Cu reaction remained practically unaffected.

Kelly et al.<sup>51)</sup> studied the effects of two additives, sodium dodecyl sulfate (SDS) and saccharin, on the composition and microstructure of pulse-plated Cu-Co alloys. The additive SDS appeared to promote the displacement of Co by Cu during pulse off-times in the pulsed deposition of Cu-Co alloys. For short pulse periods, films made with SDS only were composed of Co-rich columns surrounded by a Cu-rich matrix phase. Films made with both SDS and saccharin at short pulse periods were face-centered cubic in orientation with a grain size of about 10-15 nm. The interfacial planarity of laminated films produced at longer pulse periods was improved by saccharin. By taking advantage of the self-organizing Co-rich columns obtained at short pulse periods and using Cu spacer layers, it was possible to obtain three-dimensional arrays of Co-rich nanophases using a single electrolyte and no masking of lithographic processes.

Mockute and Bernotiene<sup>52)</sup> investigated the interaction of additives with the cathode and the interplay of saccharin, 2-butyne-1,4-diol and phthalimide by determination of the consumption rates ( $V_c$ ) of the additives, accumulation rates ( $V_a$ )

of the cathodic reaction products and the incorporation of sulfur and carbon in electrodeposits. The main transformation products of saccharin were benzamide, *o*-toluene sulphonamide and benzylsulfate, while phthalimide gave rise to phthalimidine and *o*-toluene amide. Cathodic reaction products showed the adsorption modes of the additives on electrodeposits. Saccharin and phthalimide in the mixture increased  $V_2$  as well as  $V_a$  of *o*-toluene sulfonamide and phthalimidine. 2-Butyne-1, 4-diol decreased  $V_a$  of *o*-toluene sulfonamide and phthalimidine and increased the  $V_a$  of benzamide and incorporation of sulfur. The increase of  $V_c$  and  $V_a$  showed a synergistic effect of the additives. The aromatic compounds in the mixture under study increased additive adsorption by the carbonyl group and 2-butyne-1, 4-diol increased the adsorption of saccharin by the sulfonfyl group.

Mohanty et al.<sup>53)</sup> investigated the effects of pyridine and its derivatives on current efficiency, surface morphology and crystallographic orientations of electrodeposited nickel from acidic sulfate solutions. The results indicated that the presence of pyridine and picolines had no significant effect on current efficiency. The deposits obtained were smoother, more compact and uniform with picolines than with pyridine. A significant change in surface morphology of the electrodeposits was observed and picolines were found to be better additives than pyridine, 4-picoline being the best. X-ray diffraction revealed that the (200) plane was the most preferred plane and was not affected by the presence of any of these additives in the electrolyte.

Golodnitsky et al.<sup>54)</sup> showed that the composition of the electrodeposited nickel-cobalt alloy in

sulfamate electrolytes containing anion additives was influenced in a complicated manner by the concentrations of cobalt(II) ion and citric acid, pH, and applied current density. The operating conditions were found under which the increase in the pH of the solution adjacent to the cathode was inhibited. Citrate anions formed a wide variety of complexes with nickel and cobalt. Protonated citrate complexes of nickel(II) and cobalt(II) were apt to be involved in the electrochemical alloying process. Acetate anions served to buffer the sulfamate solutions. Nickel-cobalt electrochemical alloying lead to an increase in the reaction rate of cobalt at the expense of the nickel reaction rate. The data confirmed that inhibition of the more noble metal by the less noble one did not depend on the anion composition of the electrolyte.

Akiyama et al.<sup>55)</sup> investigated the role of polyethylene glycol (PEG) as an additive in the electrodeposition of zinc-chromium alloys in sulfate baths containing trivalent chromium. PEG with high molecular weight enabled the codeposition of metallic chromium with zinc, while chromium(III) was present in the deposits obtained from the baths containing PEG with lower molecular weight as well as the PEG-free bath.

Carlos et al.<sup>56)</sup> studied the influence of glycerol on the cathodic process of lead electrodeposition and, on its morphology. Glycerol reduced the dendritic growth but did not favor the adherence of the electrodeposits.

## FUTURE DIRECTION

Application of ionic liquids in electrodeposition will draw continued interest and research should

be continued on wider application of ionic liquids. In the near future, many new materials can be prepared by electrodeposition of composites. Pulse current plating technology will gain more importance in the future. Particularly in the electronic industry, this technology would yield improved deposit quality and step coverage for coating high aspect ratio trenches. In addition to traditional metal and alloy deposition, compound deposition could play important role and effects of various additives should be investigated continuously.

#### ACKNOWLEDGEMENT

This work was made possible for one of the author (Dr. Kim) by the professor's research abroad program of the University of Ulsan. We also thank financial support from National Science Foundation and Center for Green Manufacturing, ACIPCO, and the University of Alabama.

#### References

1. B. Wu, R. G. Reddy, and R. D. Rogers, *Light Metals 2001*, ed. J. L. Anjier, TMS (2001), pp. 237-243.
2. B. Wu, R. G. Reddy, and R. D. Rogers, *Recycling of Metals and Engineered Materials*, ed. D. L. Stewart, Jr., J. C. Daley and R. L. Stephens, TMS (2000), pp. 845-856.
3. Q. Liao, R. William, G. Stewart, C. L. Hussey, and G. R. Stafford, *J. Electrochem. Soc.* 144, 3 (1997), pp.936-943.
4. P. Chen, M. Lin, W. Sun, *J. Electrochem. Soc.* 147, 9 (2000), pp. 3350-3355.
5. S. K. Kim and H. J. Yoo, *Surf. Coat. Technol.*, 108 - 109 (1998), pp.564-569.
6. Z. Guo and X. Zhu, *J. Mat. Sci. Technol.*, 16, 3 (2000), pp. 323-326.
7. P. Nowak, R. P. Socha, M. Kaisheva, J. Fransaer, J.-P. Celis, and Z. Stinoy, *J. Appl. Electrochem.*, 30, 4 (2000), pp. 429-437.
8. L. Zhu and W. Li, *J. Func. Matls.*, 31, 1 (1999), pp. 85-87.
9. A. Moeller and H. Hahn, *Nanostructured Materials*, 12, 1 (1999), pp. 259-262.
10. B. Mueller and H. Ferkel, *Materials Science Forum ISMANAM-99 : The Int. Symp. On Metastable, Mechanically Alloyed and Nanocrystalline Materials*, v.343 (1999), pp. 476-481.
11. K. Barmak, S. W. Banovic, H. M. Chan, L. E. Friedersdorf, M. P. Harmer, A. R. Marder, C. M. Petronis, D. G. Puerta and D. F. Susan, *Electrochemical Synthesis and Modification of Materials*, *Proceeding of the 1996 MRS Fall Meeting, IEE-MRS*, v. 451 (1997), pp. 469-474.
12. J. A. Switzer, E. W. Bohannon, T. D. Golden, C. Hung, L. Hung, and M. Shumsky, *Electrochemical Synthesis and Modification of Materials*, *Proceeding of the 1996 MRS Fall Meeting, IEE-MRS*, v. 451 (1997), pp. 283-288.
13. M. Onoda, K. Shimizu, Y. Tateishi, and T. Watanabe, *Trans. Inst. Metal Fin.*, 77, 1 (1999), pp. 44-48.
14. B. Bozzini, G. Giovannelli, and P. L. Cavallotti, *J. Appl. Electrochem.*, 29, 6 (1999), pp. 685-692.
15. N. M. Teterina and G. V. Khaldev, *Zashchita Metallov*, 34, 3 (1998), pp.314-318.
16. C. Filiatre and L. Towarnicki, *J. Appl. Electro-*

- chem, 29, 12 (1999), pp. 1393-1400.
17. D. Varadarajan, C. Y. Lee, A. Krishnamoorthy, D. J. Duquette, and W. N. Grill, *J. Electrochem. Soc.*, 147, 9 (2000), pp. 3382-3392.
18. R. Blake, D. DeSalvo, and R. Retallick, *Printed Circuit Fabrication*, 23, 1 (2000) p. 274-280.
19. S. K. Ghosh, A. K. Grove, G. K. Dey, and M. K. Totlani, *Surf. Coat. Technol.*, 126, 1, (2000), pp. 48-63.
20. C. N. Panagopoulos, V. D. Papachristos, U. Wahlstrom, P. Leisner, and L. W. Christoffersen, *Scripta Materials*, 44, 7 (2000), pp. 677-683.
21. C. R. Tomachuk, C. M. de A. Freire, M. Ballester, R. Fratesi, and G. Roventi, *Surf. Coat. Technol.*, 122, 1, (1999), pp. 6-9.
22. A. Robin and R. B. Ribeiro, *J. Appl. Electrochem.*, 30, 2 (2000), pp.239-246.
23. G. Ett and E. J. Pessine, *Electrochimica Acta*, 44, 17 (1999), pp.2859-2870.
24. A. L. Portela, G. I. Lacconi and M. L. Teijelo, *J. Electroanal. Chem.*, 495, 2 (2001), pp. 169-172.
25. T. P. Moffat, J. E. Bonevich, W. H. Huber, A. Stanishevsky, D. R. Kelly, G. R. Stafford and D. Josell, *J. Electrochem. Soc.*, 147, 12 (2000), pp. 4524-4535.
26. M. Georgiadou, D. Veyret, R. L. Sani and R. C. Alkire, *J. Electrochem. Soc.*, 148, 1 (2001), pp. C54-C58.
27. S. Arai, Y. Funaoka, N. Kaneko and N. Shinohara, *Electrochim.*, 69, 5 (2001), pp. 319-323.
28. F. Ebrahimi and A. J. Liscano, *Mat. Sci. Eng. A*, 301, 1 (2001), pp. 23-34.
29. S. Shawki and S. Mikhail, *Mat. Manufac. Proc.*, 15, 5 (2000), pp. 737-746.
30. T. Yamasaki, *Script. Mat.*, 44, 8-9 (2001), pp. 1497-1502.
31. S. Goldbach, R. de Kermadec and F. Lapique, *J. Appl. Electrochem.*, 30, 3 (2000), pp. 277-284.
32. M. Donten, H. Cesiulis and Z. Stojek, *Electrochim. Acta*, 45, 20 (2000), pp. 3389-3396.
33. M. J. Giz, S. C. Bento and E. R. Gonzalez, *Int. J. Hydrogen Energy*, 25, 7 (2000), pp. 621-626.
34. Y. Zhuang and E. J. Podlaha, *J. Electrochem. Soc.*, 147, 6 (2000), pp. 2231-2236.
35. E. Barrera, M. P. Pardave, N. Batina and I. Gonzalez, *J. Electrochem. Soc.*, 147, 5 (2000), pp. 1787-1796.
36. M. Nikolova, N. Atanassov, J. Fischer-Buhrer, A. Zielonka, *Trans. Inst. Metal Fin.*, 78, 4 (2000), pp. 147-151.
37. E. Gomez, A. Llorente and E. Valles, *J. Electroanal. Chem.*, 495, 1 (2000), pp. 19-26.
38. G. Tourillon, L. Pontouier, J. P. Levy and V. Langlais, *Electrochem. Solid-State Letters*, 3, 1 (2000) pp. 20-23.
39. M. Masuda, H. Takenishi and A. Katagiri, *J. Electrochem. Soc.*, 48, 1 (2001), pp. C59-C64.
40. J. Gong and E. J. Podlaha, *Electrochem. Solid-State Letters*, 3, 9 (2000), pp. 422-425.
41. C. Lepiller, P. Cowache, J. F. Guillemoies, N. Gipson, E. Ozsan and D. Lincot, *Thin Solid Fims*, 361 (2000), pp. 118-122.
42. S. D. Thompson, L. R. Jordan and M. Forsyth, *Electrochim. Acta*, 46, 10-11 (2001), pp. 658-663.
43. M. E. Baumgaertner and D. R. Gabe, *Trans. Inst. Metal Fin.*, 78, 1 (2000), pp. 11-16.
44. A. Durairajan, B. S. Haran, R. E. White and B. N. Popov, *J. Electrochem. Soc.*, 147, 12 (2000), pp. 4507-4511.

45. C. Cao, H. Wang and H. Zhu, *Diamond and Related Mat.*, 9, 9 (2000), pp. 1786-1789.
46. A. Albu-Yaron, C. Levy-Clement, A. Katty, S. Bastide and R. Tenne, *Thin Solid Films*, 361 (2000), pp. 223-228.
47. S. Nakamura and A. Yamamoto, *Solar Energy Mat. and Solar Cells*, 65, 1 (2001), pp. 79-85.
48. R.-S. Juang and L.-C. Lin, *Sep. Sci. and Technol.*, 35, 7 (2000), pp. 1087-1098.
49. L. Muresan, S. Varvara, G. Maurin and S. Dorneanu, *Hydromet.*, 54, 2 (2000), pp. 161-169.
50. M. Scendo and J. Malyszko, *J. Electrochem. Soc.*, 147, 5 (2000), pp. 1758-1762.
51. J. J. Kelly, P. E. Bradley and D. Landolt, *J. Electrochem. Soc.*, 147, 8 (2000), pp. 2975-2980.
52. D. Mockute and G. Bernotiene, *Surf. Coat. Technol.*, 135, 1 (2000), pp. 42-47.
53. U. S. Mohanty, B. C. Tripathy, P. Singh and S. C. Das, *J. Appl. Electrochem.*, 31, 5 (2001), pp. 579-583.
54. D. Golodnitsky, N. V. Gudin and G. A. Volyanuk, *J. Electrochem. Soc.*, 147, 11 (2000), pp. 4156-4163.
55. T. Akiyama, S. Kobayashi, J. Ki, T. Ohgai and H. Fukushima, *J. Appl. Electrochem.*, 30, 7 (2000), pp. 817-822.
56. I. A. Carlos, M. A. Malaquias, M. M. Oizami and T. T. Matsuo, *J. Power Source*, 92, 1-2 (2001), pp. 56-64.